Intracellular reactive oxygen species are required for directional migration of resident and bone marrow-derived hepatic pro-fibrogenic cells

Erica Novo[1, †], Chiara Busletta[1, †], Lorenzo Valfrè di Bonzo[1], Davide Povero[1], Claudia Paternostro[1], Katia Mareschi[2, 3], Ivana Ferrero[2, 3], Ezio David[4], Cristiana Bertolani[5], Alessandra Caligiuri[5], Stefania Cannito[1], Elena Tamagno[1], Alessandra Compagnone[1], Sebastiano Colombatto[1], Fabio Marra[5], Franca Fagioli[2], Massimo Pinzani[5], Maurizio Parola[1,]

doi:10.1016/j.jhep.2010.09.022

Background & Aims

Liver fibrogenesis is sustained by myofibroblast-like cells originating from hepatic stellate cells (HSC/MFs), portal fibroblasts or bone marrow-derived cells, including mesenchymal stem cells (MSCs). Herein, we investigated the mechanistic role of intracellular generation of reactive oxygen species (ROS) and redox-sensitive signal transduction pathways in mediating chemotaxis, a critical profibrogenic response for human HSC/MFs and for MSC potentially engrafting chronically injured liver.

Methods

Intracellular generation of ROS and signal transduction pathways were evaluated by integrating morphological and molecular biology techniques. Chemokinesis and chemotaxis were evaluated by wound healing assay and modified Boyden's chamber assay, respectively. Additional *in vivo* evidence was obtained in human specimens from HCV-related cirrhosis.

Results

Human MSCs and HSC/MFs migrate in response to a panel of polypeptide chemoattractants and extracellularly generated superoxide anion. All polypeptides induced a NADPH-oxidase-dependent intracellular rise in ROS, resulting in activation of ERK1/2 and JNK1/2. Moreover, menadione or 2,3-dimethoxy-1,4-naphthoquinone, which generate intracellular superoxide anion or hydrogen peroxide, respectively, induced ERK1/2 and

JNK1/2 activation and migration. JNK1 activation was predominant for migration as shown by specific silencing. Finally, activation of ERK1/2 and JNK1/2 was found in extracts obtained from HSC/MFs during the course of an oxidative stress-mediated model of liver injury and phosphorylated JNK1/2 isoforms were detected in α-smooth muscle actin-positive myofibroblasts lining fibrotic septa in human cirrhotic livers.

Conclusions

Intracellular generation of ROS, through activation of specific signaling pathways, is a critical event for directional migration of HSC/MFs and MSCs.

Abbreviations

HSC/MFs, hepatic stellate cells; MSCs, mesenchymal stem cells; ROS, reactive oxygen species; ERK1/2, extracellular regulated kinase 1/2; CLDs, chronic liver diseases; JNK1/2, c-Jun N-terminal kinase isoforms 1/2; MEN, menadione; DMNQ,2,3-dimethoxy-1,4-naphtoquinone; MFs, myofibroblast-like cells; EMT, epithelial to mesenchymal transition; PDGF, platelet-derived growth factor; MCP-1 or CCL2,monocyte chemoattractant protein-1; AT-II, angiotensin II; VEGF, vascular endothelial growth factor; α-SMA, smooth muscle actin alpha; CCl_4, carbon tetrachloride; rATF2,activating transcription factor-2; DCFH-DA, 2′,7′-dichlorodihydrofluorescein diacetate;H_2O_2, hydrogen peroxide; HNE, 4-hydroxynonenal; DAPI, 4,6-diamino-2-phenyilindole;HCV, hepatitis C virus; HGF, hepatocyte growth factor; bFGF, basic fibroblast growth factor; SDF-1 or CXCL12, stromal cell-derived factor 1; X/XO, xanthine–xanthine oxidase; NsC, non-silencing siRNA; MEFs, mouse embryo fibroblasts; DPI,diphenylphenylene-iodonium; HO-1, heme oxygenase 1

Keywords

Hepatic stellate cells; Mesenchymal stem cells; Liver fibrogenesis; Reactive oxygen species; Chemotaxis

Introduction

Fibrotic progression of chronic liver diseases (CLDs) is sustained by hepatic populations of myofibroblast-like cells (MFs) that originate mainly from activation of hepatic stellate cells (HSC) and portal (myo)fibroblasts [1], [2], [3], [4] and [5] or, to a lesser extent, through epithelial to mesenchymal transition (EMT) of hepatocytes and/or cholangiocytes [3], or circulating and bone marrow-derived mesenchymal stem cells (MSCs) or fibrocytes [4] and [5] engrafting chronically injured liver. Most of our knowledge derives from studies on fully activated, MF-like HSC (HSC/MFs) and their phenotypic responses (proliferation, increased synthesis of ECM, and pro-inflammatory mediators, migration, contractility) that are initiated and/or sustained by growth factors, chemokines, adipokines [1], [2], [3], [4] and [5], reactive oxygen species (ROS), and other mediators [6]. Whatever their origin be, MFs ability to migrate towards the site of injury and to align with nascent and established fibrotic septa represents a relevant pro-fibrogenic feature which, in turn, may be critical in recruiting circulating MSCs and driving their migration once differentiated into a MF-like phenotype. Induction of HSC/MFs chemotaxis is stimulated by polypeptides overexpressed during CLDs, including platelet-derived growth factor (PDGF), monocyte chemoattractant protein-1 (MCP-1 or CCL2) [7], angiotensin II (AT-II) [8], vascular-endothelial growth factor (VEGF), angiopoietin-1 [9], and ROS like superoxide anion [10] and [11]. PDGF, the best characterized and most potent chemoattractant for HSC/MFs, is also active on human MSC in their fibroblast-like and α-SMA-positive phenotype [12]. Moreover, chemoattractants operate by activating Ras/ERK signaling, with only PDGF being able to activate PI-3 K/c-Akt signaling [1], [2],[6], [7], [8], [9], [10], [11] and [12].

In this study, we show that all effective stimuli for profibrogenic human HSC/MFs and bone marrow-derived fibroblast-like MSCs require, as a common critical step, intracellular generation of ROS in order to trigger chemotaxis through a mechanism that involves redox-sensitive activation of ERK1/2 and JNK1/2.

Materials and methods

Materials

Human recombinant growth factors and cytokines were from PeproTech Inc. (Rocky Hill, NJ). Monoclonal and polyclonal antibodies against phosphorylated and unphosphorylated ERK1/2 or JNK1/2 were from Santa Cruz Biotechnology (Santa Cruz, CA) or Cell Signaling Technology (Beverly, MA), respectively. SP600125 and PD98095 were from Calbiochem (La Jolla, California, USA). Male adult Wistar rats were from Harlan-Nossan (Correnzana, Italy). The enhanced chemiluminescence reagents and nitrocellulose membranes (Hybond-C extra) were from Amersham Pharmacia Biotech (Milano, Italy). All other reagents were from Sigma Aldrich Spa (Milan, Italy).

Isolation and culture of hepatic stellate cells and mesenchymal stem cells

Human HSC were isolated and characterized [13] from surgical wedge sections of at least three different human livers not suitable for transplantation after obtaining the approval of the Human Research Review Committee (University of Florence). HSC were cultured as previously described [9] and [11], used between passages 4 and 7 (fully activated HSC/MFs), plated to obtain the desired sub-confluence level, and then left for 24 h in serum-free Iscove's medium to have cells at the lowest level of spontaneous proliferation. Procedures for isolation of rat HSCs have also been extensively described[14].

Bone marrow cells were obtained from human donors after informed consent. Aliquots of 2–3 ml of whole bone marrow were seeded in MSC-medium MEM (Lonza, Versviers, Belgium) at 10% of fetal bovine serum and cultured for 5 days. Adherent cells, when at confluence, were detached by Trypsin/EDTA, seeded at 1000/cm^2, expanded, and used for "*in vitro*" experiments from passage 3 to passage 7, when displaying a fibroblast-like and α-SMA positive phenotype [12]. Immunophenotypic analysis of hMSCs and their differentiative potential have been described elsewhere [12] and [15]. MSCs used were always more than 90% positive (cytofluorimetric analysis) for CD90, CD73, CD105, and CD29 but negative for CD34, CD45, and CD14.

Animal experiments

Male adult Wistar rats, initial weight 200–220 g, receiving human care and with experimental protocols performed according to national and local guidelines, were fed a standard pelleted diet and water *ad libitum*. Acute liver injury was induced by single oral treatment with carbon tetrachloride (CCl_4) and animals were sacrificed from 24 to 96 h, as previously described [16].

Cell migration and chemotaxis

Non-oriented migration (chemokinesis) and chemotaxis of human HSC/MFs and human MSCs were evaluated by performing the wound healing assay (20 h of incubation) or the modified Boyden's chamber assay (6 h of incubation), as described [9], [11] and [16].

Molecular biology procedures

Total cell extracts were subjected to SDS–PAGE on 10% or 7.5% acrylamide gels. The blots were incubated with desired primary antibodies and then with peroxidase-conjugated anti-mouse or anti-rabbit immunoglobulins in Tris-buffered saline–Tween containing 2% (w/v) non-fat dry milk [9] and [16] and developed with the enhanced chemiluminescence reagents according to manufacturer's instructions.

Target siRNA sequences for down-regulation of human JNK isoforms are:

(1)

(5′-GAAAGAATGTCCTACCTTCT-3′), found in both *JNK1* mRNA (nucleotide 393–412) and *JNK2* mRNA (nucleotide 425–444) [17].

(2)

(5′-GTGGAAAGAATTGATATATAA-3′) found in *JNK1* mRNA.

(3)

(5′-AAGAGAGCTTATCGTGAACTT-3′) found in *JNK2* mRNA.

siRNAs and related non-silencing controls were synthesized by Qiagen-Xeragon (Germantown, MD, USA). For transfection, the Amaxa nucleofection technology (Amaxa;

Koln, Germany) was employed [18]. JNK1/2 protein levels were analyzed by Western blot analysis 96 h after transfection.

JNK activity in HSC lysates was detected using recombinant activating transcription factor-2 (rATF2) as substrate [19].

Detection of intracellular and *in vivo* levels of ROS

Intracellular levels of ROS were detected by means of the semi quantitative 2′,7′-dichlorodihydrofluorescein diacetate (DCFH-DA) fluorescence technique, as previously detailed [20], in cells exposed to the desired stimulus for 15 min or to 50 μM hydrogen peroxide (H_2O_2, positive control).

In vivo levels of ROS or 4-hydroxynonenal (HNE) were detected [16] and [21] on extracts obtained from the liver of control rats as well as of rats treated with a single dose of $CCl_4$and then sacrificed 24, 48 and 72 h after treatment.

Morphological analysis

Indirect immunofluorescence was performed on liver cryostat sections from human biopsies from HCV cirrhotic patients (6 μm thick), as described [9]. Final dilution of primary antibodies was 1:250 (α-SMA), 1:50 (*p*-JNK1/2). Immune-positivity was revealed by the appropriate secondary Cy3-conjugated (1:1000 dilution) or Cy2-conjugated (1:200 dilution) antibodies (Amersham Pharmacia Biotech, Milano, Italy). Nuclei were stained using 4,6-diamino-2-phenyilindole (DAPI) and slides were examined with an Olympus Fluoview 300 confocal laser scanning microscope.

Immunohistochemistry was performed on paraffin liver sections from patients with hepatitis C virus (HCV) related liver cirrhosis (METAVIR F4). The use of this material conforms to the ethical guidelines of the 1975 Declaration of Helsinki and was approved by the University of Florence Human Research Review Committee. Sections (2 μm thick) were incubated with specific antibodies raised against phosphorylated JNK isoforms or α-SMA (final dilutions 1:30 and 1:1000, respectively). Briefly, after microwave antigen retrieval, primary antibodies were labelled by using EnVision, HRP-labelled System (DAKO) antibodies directed against rabbit antigen and visualized by 3′-diaminobenzidine substrate.

Negative controls were performed by replacing the respective primary antibodies by isotype and concentrations matched irrelevant antibody.

Statistical analysis

Data in bar graphs represent means ± SEM, and were obtained from average data of at least three independent experiments. Luminograms and morphological images are representative of at least three experiments with similar results. Statistical analysis was performed by Student's *t*-test or ANOVA for analysis of variance when appropriate (p <0.05 was considered significant).

Results

Migration of human HSC/MFs and MSCs in response to chemoattractants

HSC/MFs (Fig. 1A), migrated significantly in response to PDGF-BB, MCP-1, VEGF, and superoxide anion, whereas hepatocyte growth factor (HGF), basic fibroblast growth factor (bFGF), and stromal cell-derived factor 1 (SDF-1 or CXCL12) were ineffective. Human MSCs (Fig. 1B) in their fibroblast-like phenotype migrated in response to a wider panel of stimuli including PDGF-BB, VEGF, MCP-1, X/XO, HGF, βFGF, and SDF-1. Angiotensin II (AT-II) was the only one able to elicit chemotaxis on both cell types.

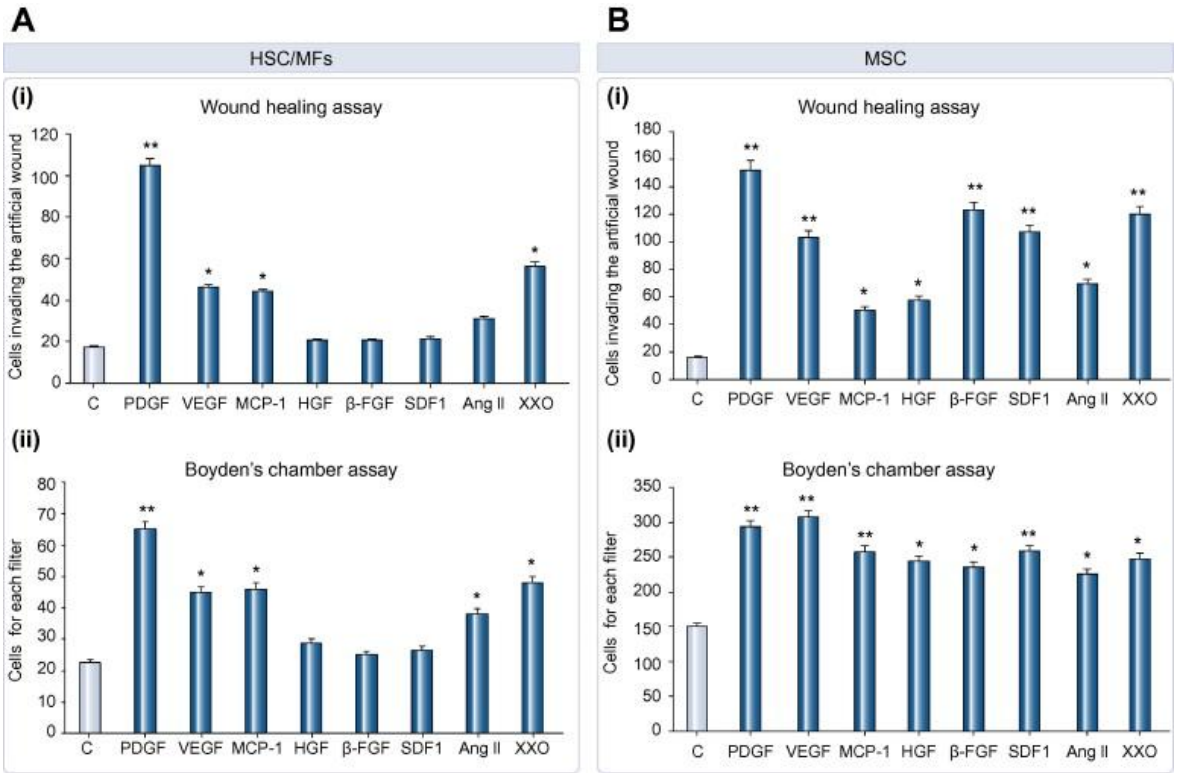

Fig. 1.

Migration of hHSC/MFs and hMSCs in response to chemoattractants. Wound healing assay (i) and chemotaxis assay (ii) were performed on hHSC/MFs (A) and hMSCs (B). Cells were either not treated (control) or treated with PDGF-BB (10 ng/ml), VEGF (100 ng/ml), MCP-1 (100 ng/ml), HGF (20 ng/ml), βFGF (20 ng/ml), SDF1 (20 ng/ml), Ang II (nM) or XXO system (0.4 mM/2 mU). Data in bar graphs represent mean ± SEM (n = 4, in triplicate) and are expressed as number of cells migrated in the artificial lesion or in the filter of Boyden's chambers. $^{*}p$ <0.05 and $^{**}p$ <0.01 versus control values.

All pro-migratory polypeptides induced an early (15 min) activation of ERK1/2 and JNK1/2 in HSC/MFs and MSCs, with increased phosphorylation of JNK1/2 being mostly limited to 46 kDa isoforms (Fig. 2 A and B).

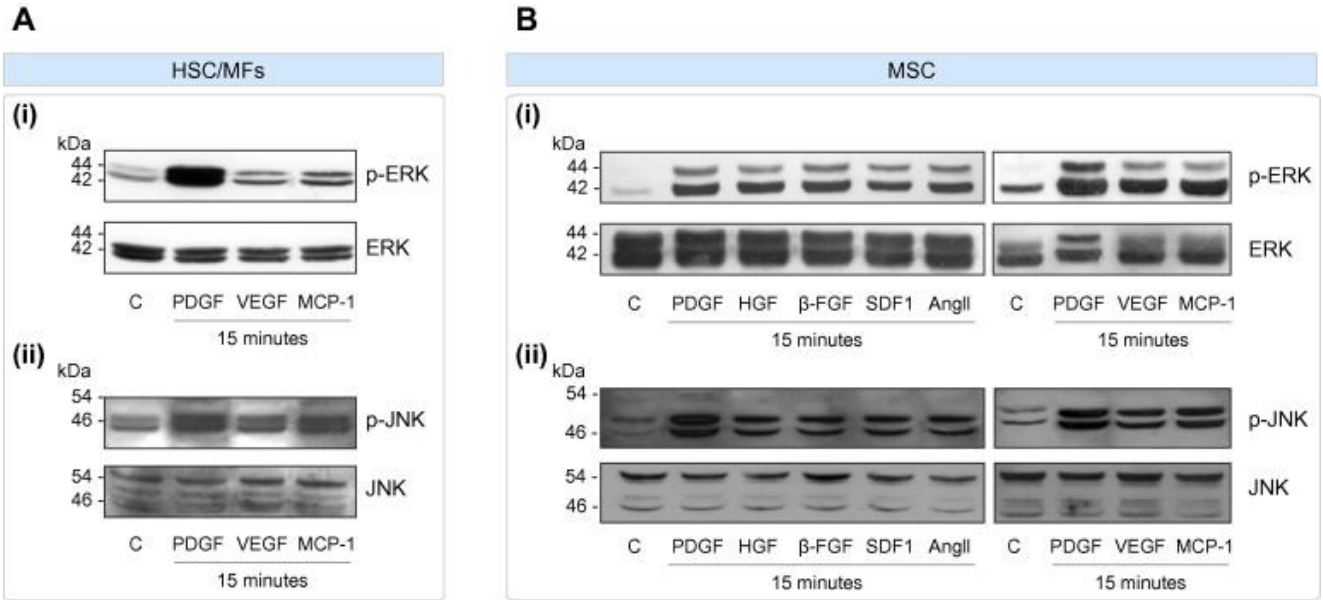

Fig. 2.

Polypeptide factors induce migration through early activation of ERK1/2 and JNK1/2. Confluent and 24-h-starved HSC/MFs (A) and hMSCs (B) were incubated for 15 min in the presence of chemoattractants. Levels of phosphorylated and unphosphorylated ERK1/2 (p44 and p42) (i) and JNK1/2 (p46 and p54) (ii) were detected in western blot analysis on total lysates by using specific antibodies.

A PDGF-BB- (used as reference chemoattractant) and time-dependent analysis of ERK1/2 and JNK1/2 phosphorylation revealed (Supplementary Fig. 1 A and B) that: (a) increased phosphorylation of ERK1/2 was detectable from 15 min until 4–6 h; (b) increased phosphorylation of 46 kDa JNK1/2 isoforms followed a biphasic pattern with an early activation detected at 15–30 min and a second peak at 2 h of incubation for HSC/MFs or afterwards for MSCs.

Based on preliminary results, PDGF-BB, MCP-1, and VEGF were used throughout the study as positive stimuli to investigate in detail the involvement of ERK1/2 and JNK1/2. Pre-treatment with PD98095, pharmacological inhibitor of ERK1/2 upstream kinase MEK-1, inhibited chemokinesis and chemotaxis in HSC/MFs, as previously reported, [6],[7], [8], [9], [10] and [11] and MSCs; similar results were obtained by pre-treating cells with the pharmacological inhibitor of JNK1/2 SP600125 (Supplementary Fig. 2A and B). In preliminary experiments we then selected an siRNA that significantly down-

regulated 46 kDa JNK1/2 isoforms in both cell types, and resulted in a significant decrease in JNK1/2 phosphorylation in response to PDGF-BB, chosen as a reference chemoattractant (Fig. 3A and B). When HSC/MFs and MSCs silenced for JNK1/2 were then exposed to PDGF-BB, VEGF, and MCP-1, chemotaxis was either significantly reduced (as for PDGF-BB) or almost abolished (Fig. 3A and B) as compared with cells carrying non-silencing siRNA (NsC). Moreover, as an additional proof of principle, experiments performed in mouse embryo fibroblasts from JNK1/2 double knock-out mice (MEF cells, Supplementary Fig. 3B) versus wild type fibroblasts revealed that only few MEF cells (15–20% in a typical experiment) migrated in response to PDGF-BB. To further explore the role of different isoforms we next employed siRNAs designed to silence JNK1 or JNK2 isoforms in both cell types and in these conditions we found that, running both WHA and chemotaxis assays in response to PDGF-BB, the contribution of JNK1 isoforms to migration was more significant (Fig. 3C and D).

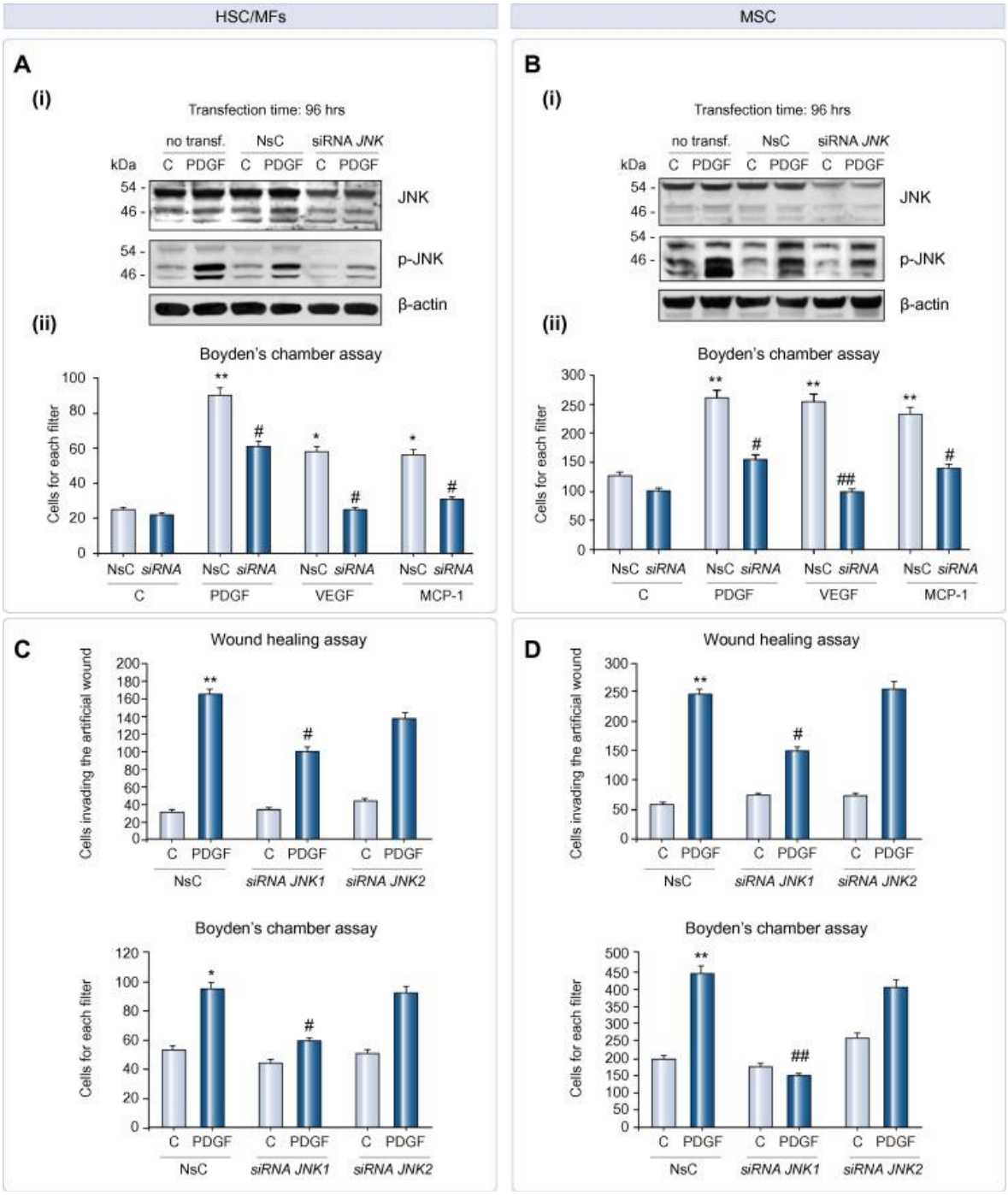

Fig. 3.

JNK1/2 silencing inhibited polypeptide-dependent chemotaxis. hHSC/MFs (A and C) or hMSCs (B and D) were silenced for *JNK1/2* (A and B) or for the single *JNK1* or JNK2 isoforms (C and D). Total cell lysates (i) from JNK1/2 silenced hHSC/MFs (A) or hMSCs (B), or cells transfected with a non-silencing control siRNA (NsC) were used in western blot analysis to evaluate phosphorylated and unphosphorylated JNK1/2 levels 96 h after transfection in

cells treated or not with PDGF-BB, used as positive control. Chemotaxis (A–D) and chemokinesis (C and D) were always assessed in cells not transfected, cells transfected with NsC, and cells transfected with the desired siRNA. Cells were then either not treated (control cells) or treated with the indicated polypeptides (same concentrations as in Fig. 1 legend). Data are expressed as number of cells migrated in the artificial lesion or in the filter of Boyden's chambers. Data in bar graphs represent mean ± SEM (n = 3, in triplicate) and are expressed as number of cells migrated in the artificial lesion or in the filter of Boyden's chambers. $^{*}p$ <0.05 and $^{**}p$ <0.01 versus control values. $^{\#}p$ <0.01 and $^{\#\#}p$ <0.05 versus values in cells stimulated with polypeptide factors.

Migration induced by polypeptide growth factors critically requires intracellular generation of ROS

We next performed experiments to investigate whether intracellular generation of ROS may be critical in our experimental conditions. Preliminary experiments (Supplementary Fig. 4) performed with the pharmacological inhibitor of NADPH-oxidase diphenylphenylene-iodonium (DPI) indicated that: (a) DPI significantly inhibited or abolished chemokinesis and chemotaxis stimulated by PDGF-BB, MCP-1, and VEGF in HSC/MFs and MSCs; (b) DPI reduced phosphorylation of both ERK1/2 and JNK 46 kDa isoforms induced by PDGF-BB, was used as positive control. By employing the DCFH-DA semi-quantitative morphological technique, PDGF-BB, VEGF, and MCP-1 all induced an early (within 15 min) and significant increase in ROS-related intracellular fluorescence (Fig. 4A and B), a finding significantly prevented by pre-treating cells with the more specific NADPH-oxidase pharmacological inhibitor apocynin (Fig. 4C and D). Accordingly, apocynin also significantly inhibited polypeptide-induced chemokinesis and chemotaxis in HSC/MFs (Fig. 5A) and in MSCs (Fig. 5B). DPI and apocynin, at the experimental dose used, were completely ineffective on parameters of either necrotic or apoptotic cell death (Supplementary Fig. 4C and D).

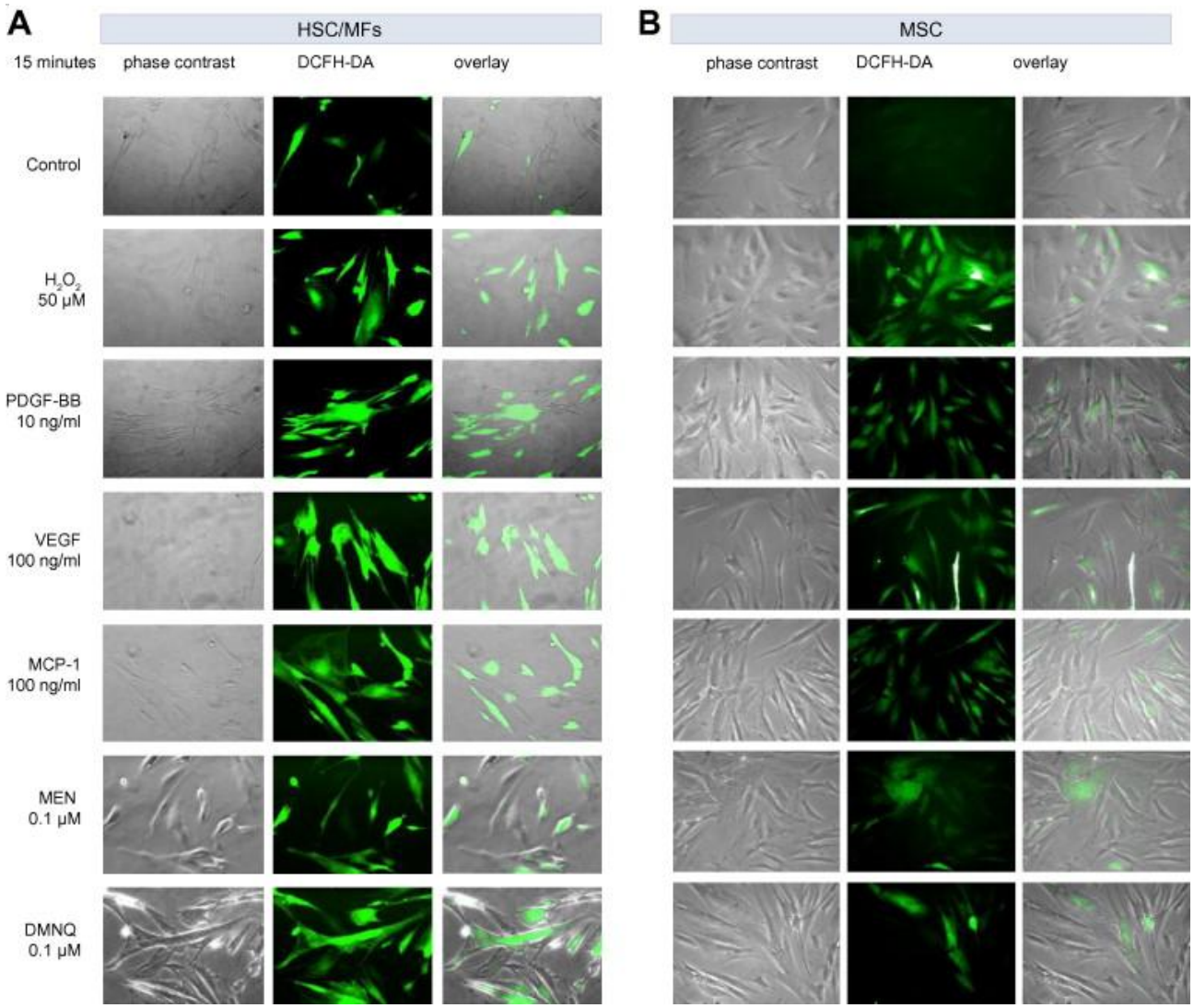

Fig. 4.

Intracellular generation of ROS in cells exposed to chemoattractants. Generation of intracellular ROS (green fluorescence) was detected by the semi-quantitative technique based on the use of DCFH-DA at 15 min in control cells, HSC/MFs (A) and MSCs (B) treated with PDGF-BB (10 ng/ml), VEGF (100 ng/ml), MCP-1 (100 ng/ml), Menadione (0.1 µM), DMNQ (0.1 µM) or H2O2 (50 µM), the latter used as positive control. When required, cells were pre-treated for 1 h with apocynin 100 µM (C and D). For any condition, three images are offered of the same field representing phase contrast image (left column), DCFH-DA positive fluorescence (middle column), and their digital overlay (right column).

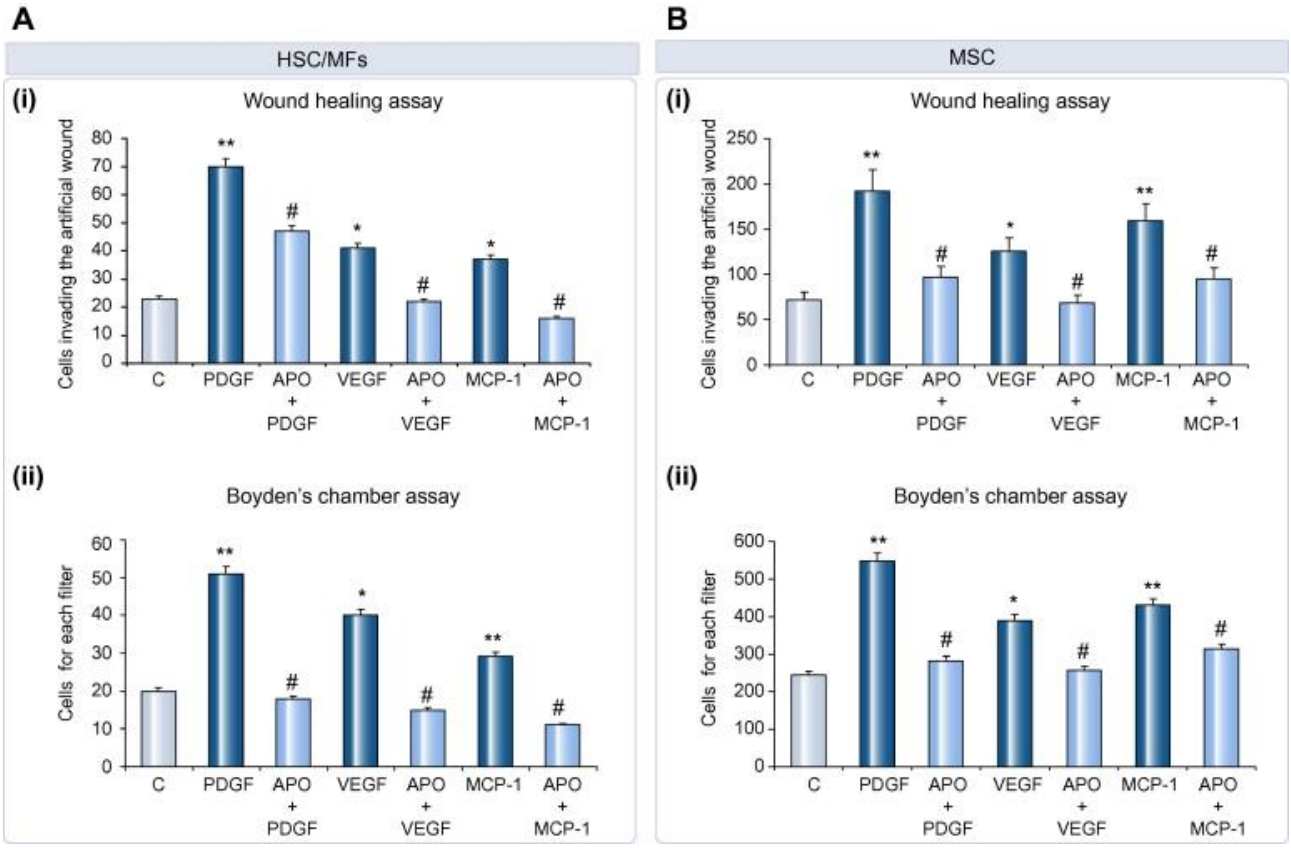

Fig. 5.

Polypeptide-dependent migration required intracellular ROS production. Wound healing assay (i) and chemotaxis assay (ii) were performed on (A) hHSC/MFs and (B) hMSCs cells not exposed (control cells) or treated with VEGF (100 ng/ml), MCP-1 (100 ng/ml) or PDGF-BB (10 ng/ml) and, when required, pre-treated for 1 h with apocynin (100 μM). Data in bar graphs represent mean ± SEM (n = 4, in triplicate) and are expressed as number of cells migrated in the artificial lesion or in the filter of Boyden's chambers. $^{*}p$ <0.05 and $^{**}p$ <0.01 versus control values. $^{\#}p$ <0.01 and $^{\#\#}p$ <0.05 versus values in cells stimulated with polypeptide factors.

Polypeptide-independent intracellular generation of ROS is sufficient to induce ERK1/2 and JNK1/2 activation and migration

In order to characterize the role of ROS in triggering migration, we employed 2-methyl-1,4-naphthoquinone (Menadione, MEN) and 2,3-dimethoxy-1,4-naphthoquinone (DMNQ),

which are known to induce in target cells a significant intracellular generation of superoxide and H_2O_2, respectively. In preliminary experiments, we found that 10 µM concentrations of MEN and DMNQ induced in HSC/MFs evident morphological changes or changes in LDH release or caspase 3 activation (Supplementary Fig. 5A–C). Since homologous results were found for MSCs (data not shown) MEN and DMNQ were employed in all experiments at 0.1 µM, a non-toxic dose resulting in intracellular generation of ROS in both cell types (Fig. 4A and B).

Exposure of HSC/MFs and MSCs to MEN or DMNQ triggered an early and significant increased phosphorylation of ERK1/2 and JNK1/2 (Fig. 6A and B) as well as chemokinesis and chemotaxis that were again prevented by PD98095 (Supplementary Fig. 6A and B). Moreover, in cells silenced for JNK1/2 chemotaxis stimulated by MEN and DMNQ was significantly decreased (Fig. 6C and D), as compared to cells transfected with a non-silencing RNA (NsC).

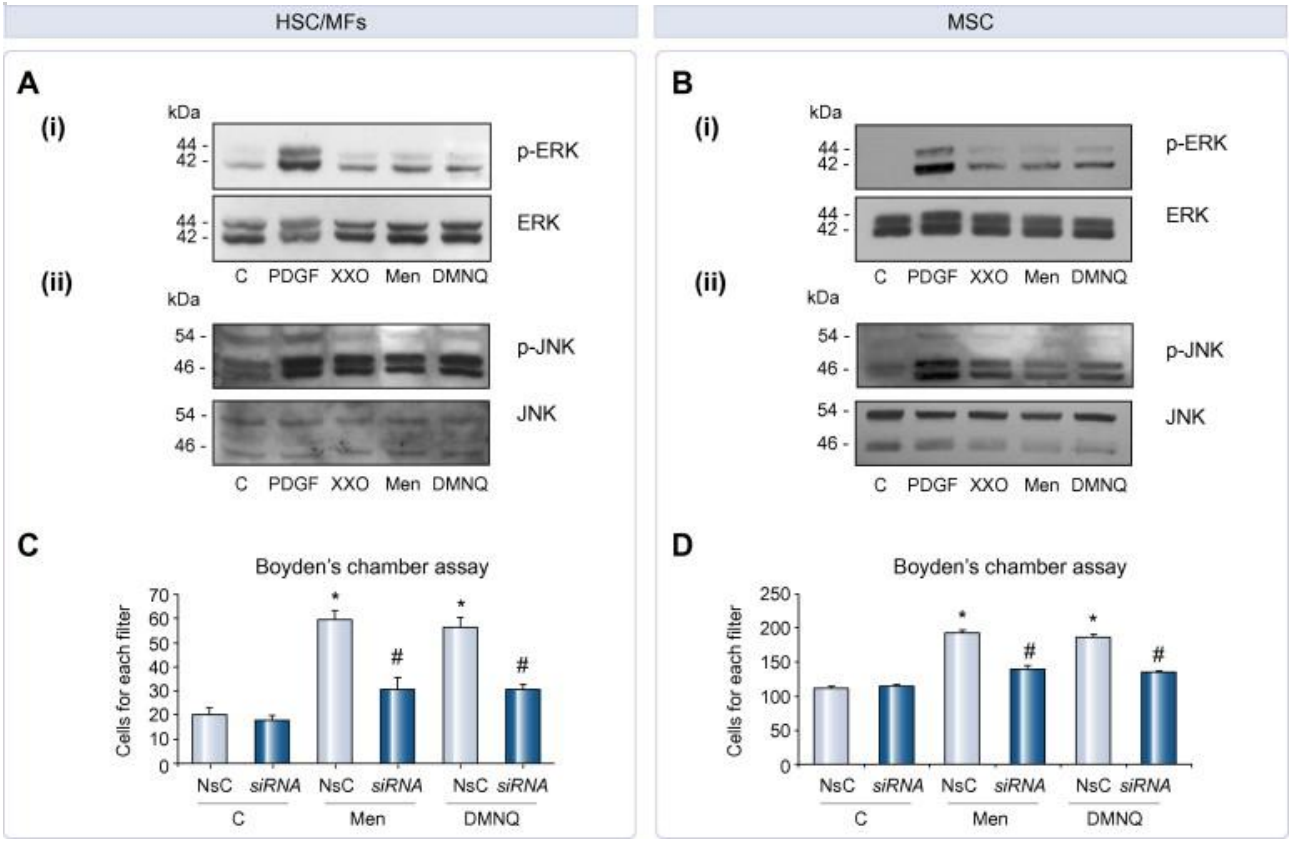

Fig. 6.

ROS-dependent migration was associated with activation of ERK1/2 and JNK1/2. Confluent and 24-h-starved (A) HSC/MFs and (B) MSCs were exposed to PDGF-BB (10 ng/ml), Menadione (0.1 μM), DMNQ (0.1 μM), and XXO system (0.4 mM/2 mU). Total cell lysates were used in Western blotting to detect phosphorylated and unphosphorylated ERK1/2 (p44 and p42) (i) and JNK1/2 (p46 and p54) (ii) isoforms. Chemotaxis was assessed on (C) HSC/MFs or (D) MSCs that were either untransfected, transfected with NsC or with *JNK1/2* siRNA and finally not treated (control cells) or treated with Menadione or DMNQ. Data in bar graphs represent mean ± SEM (n = 4, in triplicate) and are expressed as number of cells migrated in the filter of Boyden's chambers. $^{*}p$ <0.05 versus control values. $^{\#}p$ <0.01 versus values in cells stimulated with Menadione and DMNQ.

Increased generation of ROS and JNK activity *in vivo*

In order to evaluate whether intracellular generation of ROS and JNK activation were likely to occur *in vivo*, activation of JNK1/2 was first investigated in cell extracts obtained from freshly isolated rat HSC obtained at different time points after administration of a single dose of CCl_4, a model of acute liver injury in which oxidative stress is up-regulated from early time points (2–6 h) to 48–72 h [17] and [19], as shown by hepatic levels of ROS and 4-hydroxynonenal (Fig. 7A and B). HSC lysates from CCl_4-injured livers, in which activation of ERK1/2 was already reported [22], were characterized by a very significant increase of JNK activity (24 h) and (6 h) heme oxygenase 1 (HO-1), a cytoprotective enzyme that is considered a marker of ongoing oxidative stress (Fig. 7 C and D). HO-1 protein levels were still elevated until 48 h and declined significantly starting from 72 h (data not shown).

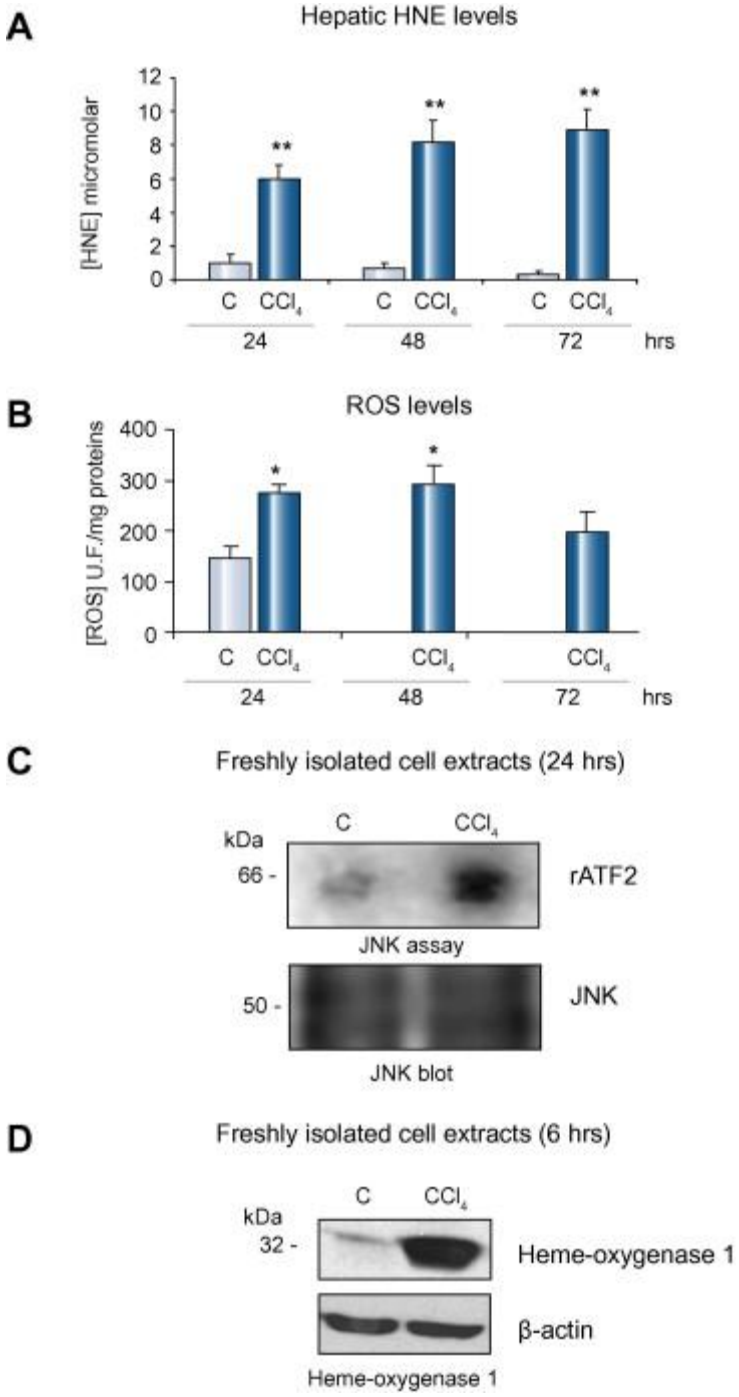

Fig. 7.

Oxidative stress"*in vivo*" was concomitant to JNK1/2 activation in HSC/MFs. *In vivo* oxidative stress was evaluated in terms of hepatic levels of (A) HNE or (B) ROS in liver samples obtained from rats receiving either CCl_4 (1.25 ml/kg b.w.) or the vehicle alone (Control) and then sacrificed after 24, 48 and 72 h. Data in bar graphs, expressed as micromolar concentration in liver tissue (HNE) or as arbitrary units of fluorescence for mg of proteins (ROS), represent mean ± SEM and are referred to six animals for any

experimental time point. $^{*}p$ <0.05 and $^{**}p$ <0.01 versus control values. (C) Total cell lysates were prepared from freshly isolated HSC obtained from rats treated with CCl_4 or vehicle alone at the indicated time point. JNK assay was performed after JNK immunoprecipitation using recombinant activating transcription factor 2 (rATF2) as a substrate (upper panel). An aliquot of the immunobeads was analyzed for JNK levels by Western blotting (lower panel). (D) Lysates were prepared as described for panel (C) and levels of HO-1 were analyzed by Western blotting (upper panel). Membranes were reblotted for β-actin to assess equal loading (lower panel).

As a second approach, immune-positivity for phosphorylated JNK isoforms (pJNKs) and α-SMA was investigated on liver specimens from chronic HCV cirrhotic patients. Immunohistochemistry showed evident *p*-JNK positive nuclear staining for cells included in α-SMA positive fibrotic septa whereas hepatocytes exhibited only faint cytoplasmic positivity (Fig. 8). Confocal laser microscopy analysis (indirect immunofluorescence on frozen specimens, Fig. 9) confirmed this scenario and was critical in showing unequivocal colocalization of *p*-JNK positive staining in several α-SMA-positive MFs within septa or at the interface between septa and parenchyma.

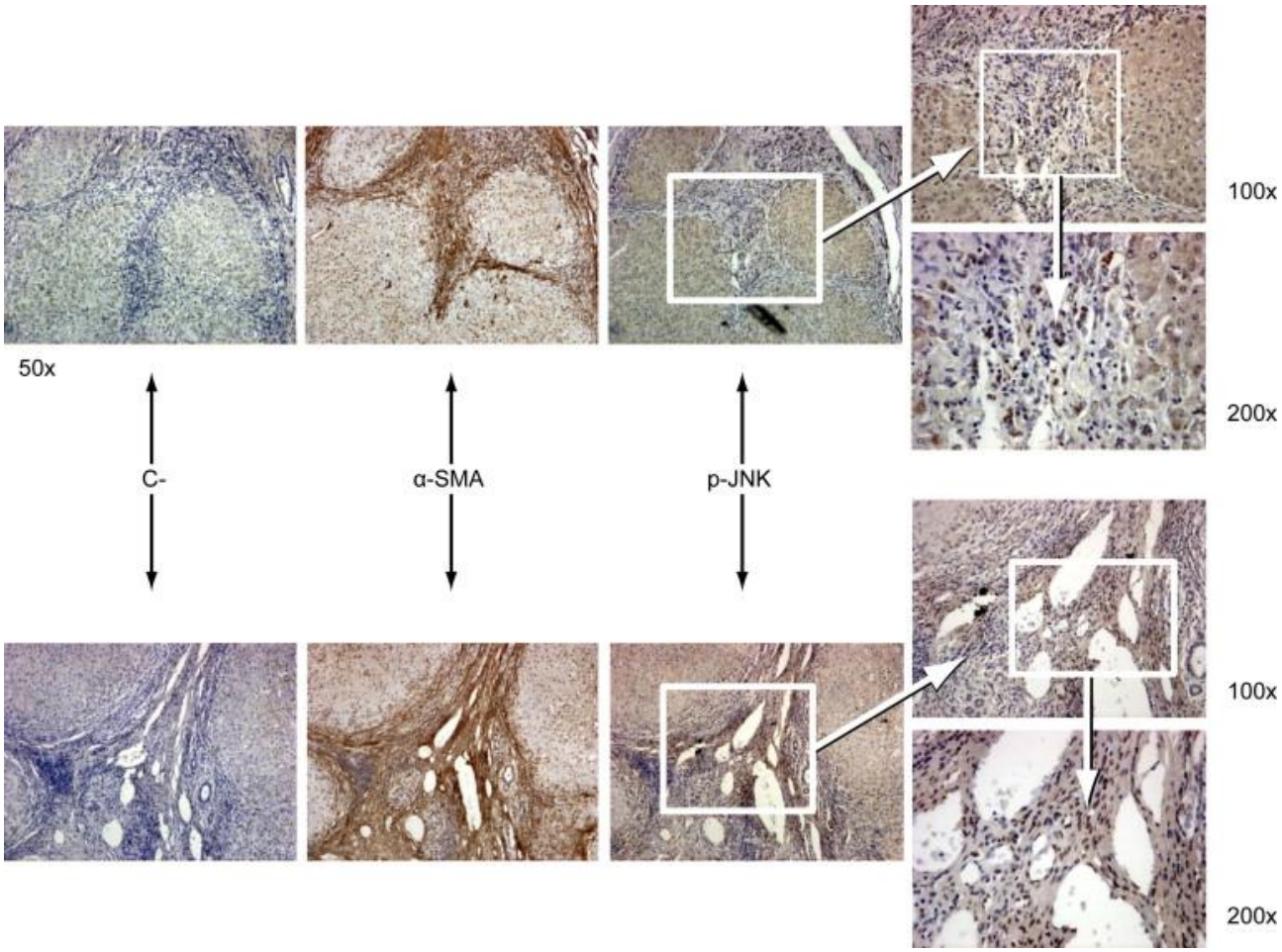

Fig. 8.

Phosphorylated JNK isoforms and α-SMA in human cirrhosis. Immunohistochemistry was performed on paraffin serial sections from patients with hepatitis C virus (HCV) related liver cirrhosis (Metavir F4) using antibodies against α-SMA or phosphorylated-JNK. Upper panels (C): negative control. Original magnification as indicated.

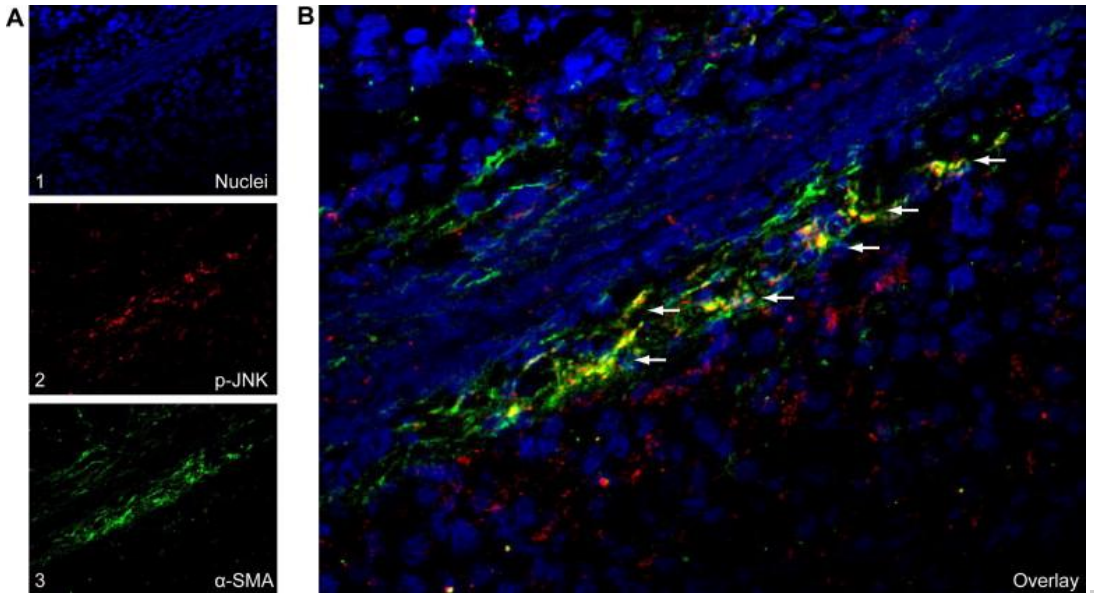

Fig. 9.

JNK1/2 activation in α-SMA positive cells in cirrhotic livers. Confocal laser microscopy was performed on liver cryostat sections from cirrhotic HCV patients. The panel includes: (A) tiny images on the left side representing image acquisition of single fluorescence identifying nuclei (1, blue fluorescence, DAPI staining), phosphorylated JNK isoforms (2, red fluorescence) and α-SMA (3, green fluorescence); (B) a larger image (overlay) offering electronic merging of fluorescent images. White arrows indicate colocalization between α-SMA and phosphorylated JNKs.

Discussion

Migration in response to chemoattractant polypeptides or other mediators generated during CLDs represents a distinctive feature of HSC/MFs and hepatic MFs of different origin [1], [2], [3], [4] and [5], leading these cells to align with inflammatory cells along fibrotic septa during fibrogenic progression. The present study provides the following major original messages: (a) intracellular generation of ROS and related activation of JNK1/2 isoforms (as for ERK1/2) are critical steps in the induction of chemotaxis in both human HSC/MFs and fibroblastic-like, α-SMA-positive human bone marrow-derived MSCs; (b) in both cell types, these common signaling mechanisms are triggered by polypeptide chemoattractants, but polypeptide-independent intracellular generation of ROS is sufficient

to trigger chemotaxis; (c) human HSC/MFs and fibroblastic-like MSCs respond to a common panel of pro-fibrogenic and pro-migratory signals generated in CLDs.

Migration of human HSC/MFs in response to chemoattractants was already reported to involve the Ras/ERK pathway [1], [3], [7], [8] and [9], with only PDGF [1], [3] and [7] being able to activate the PI-3 K/c-Akt pathway. The involvement of a more complex scenario was first suggested by studies showing that either skin fibroblasts [23] or rat HSC [24]migrated in response to PDGF-BB by a pathway involving transient activation of JNK isoforms, a scenario that our study revealed to be common to all effective polypeptide chemoattractants.

Since the involvement of the Ras/ERK pathway was already characterized in the literature, we then focused on the role of intracellular generation of ROS and of transient activation of JNK1/2. JNKs are redox sensitive serine/threonine protein kinases involved in a number of “stressful” conditions, including inflammation, differentiation, apoptosis, and insulin resistance [25] and [26] as well as in the growth factor – dependent regulation of migration and epithelial morphogenesis [27]. A mechanistic relationship between polypeptide-dependent JNK1/2 activation and migration was unequivocally shown by silencing an evolutionary conserved sequence common to both JNK1 and JNK2 isoforms or in fibroblasts obtained from mouse embryos with targeted deletion of both JNK isoforms. Since polypeptide-dependent activation of JNK1/2 was an early (within 15 min), transient (i.e., unable to induce apoptosis) and specific event, being mostly limited to 46 kDa isoforms, silencing of both JNK1 and JNK2 was the starting reasonable experimental choice because: (a) alternative splicing of JNK1 and JNK2 leads to eight different isoforms of 54 and 46 kDa, the latter molecular weight including JNK1α1, JNK1β1, JNK2α1, and JNK2β1 isoforms [25]; (b) the combined deficiency for both isoforms in double knock out mice is lethal in embryo development. However, it should be noted that under conditions of specific selective silencing, we observed that JNK1 silencing was more effective in inhibiting migration and chemotaxis, suggesting a prevalent role for JNK1 according to recent published data [28] and [29].

In our study, a critical pro-migratory role for ROS-mediated JNK activation was outlined by the following *in vitro* findings: (1) exposure of human HSC/MFs and MSCs to PDGF-BB, VEGF, MCP-1, MEN or DMNQ resulted in an early increase in intracellular ROS generation; (2) JNK1/2 activation and migration were reproduced simply by exposing cells to non-cytotoxic levels of either MEN or DMNQ, two redox-cycling chemicals able to generate intracellular superoxide anion or hydrogen peroxide, respectively; (3) polypeptide-dependent activation of JNK1/2 (and ERK1/2) by ROS and subsequent migration were prevented by inhibiting NADPH-oxidase, a ROS-generating membrane that may contribute to most of the polypeptide-induced phenotypical response of HSC/MFs [30]; (4) ROS-dependent migration was almost abolished in HSC/MFs and MSCs silenced for JNK1/2.

Human and experimental *in vivo* data further support this scenario: (1) in HCV cirrhotic human livers, positivity for phosphorylated JNK1/2 isoforms was mainly detected in α-SMA positive MFs located within fibrotic septa or at the interface between septa and parenchyma, a scenario consistent with the one reported by Kluwe et al. [29]; (2) activation of JNK1/2, preceded by up-regulation of HO-1 expression, a typical redox-sensitive gene [31], was detected at an early time point (i.e., within 24 h) in cell extracts obtained from rat HSC/MFs isolated by acutely injured livers suggesting that "*in vivo*" HSC/MFs were indeed exposed to oxidative stress.

In conclusion, migration/chemotaxis of human HSC/MFs and MSCs stimulated by polypeptides critically requires NADPH-oxidase dependent increased generation of intracellular ROS and the consequent activation of JNK1/2 isoforms in addition to activation of Ras/ERK signaling. Moreover, ROS released in the context of chronic liver injury by damaged hepatocytes or activated inflammatory cells may induce migration/chemotaxis in both cell types that have been shown to contribute to liver fibrogenesis [1], [2], [3] and [4]. The overall scenario emerging from the present study, which is fully in agreement with the recent hypothesis of JNK being involved in HSC activation and fibrogenesis [29], further suggests JNK as a common putative therapeutic target for antioxidants and/or small molecules such as protein kinase inhibitors.

Conflict of interest

The authors who have taken part in this study declared that they do not have anything to disclose regarding funding or conflict of interest with respect to this manuscript.

Acknowledgements

The financial support was received from the Ministero dell'Università e della Ricerca(MIUR, Rome – PRIN Project 2006067527, M.P.), Ministero della Salute (Ministry of Health, Rome, project: Plasticity of stem cells: a new therapeutic option for regenerative medicine, F.F., M.P.), Regione Piemonte (Torino, M.P.), Fondazione CRT (Torino, M.P.), Compagnia di San Paolo (Torino, F.F.), Italian Liver Foundation (Florence, F.M., M.Pi), Fondazione Bossolasco (Torino, E.N., S.Co), Istituto Toscano Tumori (ITT, Florence, M.Pi.).

References

[1] Friedman SL. Mechanisms of hepatic fibrogenesis. Gastroenterology 2008;134:1655–1669.

[2] Parola M, Marra F, Pinzani M. Myofibroblast-like cells in liver fibrogenesis: emerging concepts in a rapidly moving scenario. Mol Asp Med 2008;29:58–66.

[3] Choi SS, Diehl AM. Epithelial-to-mesenchymal transitions in the liver. Hepatology 2009;50:2007–2013.

[4] Kisseleva T, Brenner DA. Mechanisms of fibrogenesis. Exp Biol Med2008;233:109–122.

[5] Henderson NC, Forbes SJ. Hepatic fibrogenesis: from within and outwith. Toxicology 2008;254:130–135.

[6] Novo E, Parola M. Redox mechanisms in hepatic chronic wound healing and fibrogenesis. Fibrog Tissue Repair 2008;1:5.

[7] Pinzani M, Marra F. Cytokine receptors and signaling in hepatic stellate cells. Sem Liver Dis 2001;21:397–416.

[8] Bataller R, Schwabe RF, Choi YH, Yang L, Paik YH, Lindquist J, et al. NADPH oxidase signal transduces angiotensin II in hepatic stellate cells and is critical in hepatic fibrosis. J Clin Invest 2003;112:1383–1394.

[9] Novo E, Cannito S, Zamara E, Valfrè di Bonzo L, Caligiuri A, Cravanzola C, et al. Proangiogenic cytokines as hypoxia-dependent factors stimulating migration of human hepatic stellate cells. Am J Pathol 2007;170:1942–1953.

[10] Galli A, Svegliati-Baroni G, Ceni E, Milani S, Ridolfi F, Salzano R, et al. Oxidative stress stimulates proliferation and invasiveness of hepatic stellate cells via a MMP2-mediated mechanism. Hepatology 2005;41:1074–1084.

[11] Novo E, Marra F, Zamara E, Valfrè di Bonzo L, Caligiuri A, Cannito S, et al. Dose dependent and divergent effects of superoxide anion on cell death, proliferation, and migration of activated human hepatic stellate cells. Gut 2006;55:90–97.

[12] Valfrè di Bonzo L, Ferrero I, Cravanzola C, Mareschi K, Rustichell D, Novo E, et al. Human mesenchymal stem cells as a two-edged sword in hepatic regenerative medicine: engraftment and hepatocyte differentiation versus profibrogenic potential. Gut 2008;57:223–231.

[13] Casini A, Pinzani M, Milani S, Grappone C, Galli G, Jezequel AM, et al. Regulation of extracellular matrix synthesis by transforming growth factor beta-1 in human fat-storing cells. Gastroenterology 1993;105:245–253.

[14] Pinzani M, Gesualdo L, Sabbah GM, Abboud HE. Effects of platelet-derived growth factor and other polypeptide mitogens on DNA synthesis and growth of cultured rat liver fat-storing cells. J Clin Invest 1989;84:1786–1793.

[15] Ferrero I, Mazzini L, Rustichelli D, Gunetti M, Mareschi K, Testa L, et al. Bone marrow mesenchymal stem cells isolated from healthy donors and sporadic amyotrophic lateral sclerosis patients. Cell Transplant 2008;17:255–266.

[16] Zamara E, Novo E, Marra F, Gentilini A, Romanelli RG, Caligiuri A, et al. 4-Hydroxynonenal as a selective pro-fibrogenic stimulus for activated human hepatic stellate cells. J Hepatol 2004;40:60–68.

[17] Gururajan M, Chui R, Karuppannan AK, Ke J, Jennings CD, Bondada S, et al. CJun N-terminal kinase (JNK) is required for survival and proliferation of Blymphoma cells. Blood 2005;106:1382–1391.

[18] Novo E, Marra F, Zamara E, Valfrè di Bonzo L, Monitillo L, Cannito S, et al. Overexpression of Bcl-2 by activated human hepatic stellate cells: resistance to apoptosis as a mechanism of progressive hepatic fibrogenesis in humans. Gut 2006;55:1174–1182.

[19] Parola M, Robino G, Marra F, Pinzani M, Bellomo G, Leonarduzzi G, et al. HNE interacts directly with JNK isoforms in human hepatic stellate cells. J Clin Invest 1998;102:1942–1950.

[20] Cannito S, Novo E, Compagnone A, Valfrè di Bonzo L, Busletta C, Zamara E, et al. Redox mechanisms switch on hypoxia-dependent epithelial-mesenchymal transition in cancer cells. Carcinogenesis 2008;29:2267–2278.

[21] Zamara E, Galastri S, Aleffi S, Petrai I, Aragno M, Mastrocola R, et al. Prevention of severe toxic liver injury and oxidative stress in MCP-1-deficient mice. J Hepatol 2007;46:230–238.

[22] Marra F, Arrighi MC, Fazi M, Caligiuri A, Pinzani M, Romanelli RG, et al. Extracellular signal-regulated kinase activation differentially regulates platelet-derived growth factor's actions in hepatic stellate cells, and is induced by in vivo liver injury in the rat. Hepatology 1999;30:951–958.

[23] Amagasaki K, Kaneto H, Heldin C-H, Lennartsson J. C-Jun N-terminal kinase is necessary for platelet-derived growth factor-mediated chemotaxis in primary fibroblasts. J Biol Chem 2006;281:22173–22179.

[24] Yoshida K, Matsuzaki K, Mori S, Tahashi Y, Yamagata H, Furukawa F, et al. Transforming growth factor beta and platelet derived growth factor signal via c-Jun N-terminal kinase-dependent SMAD2/3 phosphorylation in rat hepatic stellate cells after acute liver injury. Am J Pathol 2005;166:1029–1039.

[25] Barr RK, Bogoyevitch MA. The c-Jun N-terminal protein kinase family of mitogen-activated protein kinases (JNK MAPKs). Int J Biochem Cell Biol 2001;33:1047–1063.

[26] Temkin V, Karin M. From death receptor to reactive oxygen species and c-Jun N-terminal protein kinase: the receptor-interacting protein 1 odyssey. Immunol Rev 2007;220:8–21.

[27] Xia Y, Karin M. The control of cell motility and epithelial morphogenesis by Jun kinases. Trends Cell Biol 2004;14:94–101.

[28] Kodama Y, Kisseleva T, Iwaisako K, Miura K, Taura K, De Minicis S, et al. C-Jun N-terminal kinase-1 from hematopoietic cells mediates progression from hepatic steatosis to steatohepatitis and fibrosis in mice. Gastroenterology 2009;137:1467–1477.

[29] Kluwe J, Pradere J-P, Gwak G-Y, Mencin A, De Minicis S, Österreicher CH, et al. Modulation of hepatic fibrosis by c-Jun N-terminal kinase inhibition. Gastroenterology 2010;138:347–359.

[30] De Minicis S, Bataller R, Brenner DA. NADPH oxidase in the liver: defensive, offensive, or fibrogenic? Gastroenterology 2006;131:272–275.

[31] Cederbaum AI. Cytochrome P450 2E1-dependent oxidant stress and upregulation of antioxidant defense in liver cells. J Gastroenterol Hepatol 2006;21:S22–S25.